Nuclear Instruments and Methods in Physics Research A 806 (2016) 356–359

Contents lists available at ScienceDirect

Nuclear Instruments and Methods in Physics Research A

journal homepage: www.elsevier.com/locate/nima

# Edge effect in ohmic contacts on high-resistivity semiconductors

Arie Ruzin

*Faculty of Engineering, Tel Aviv University, 69978 Tel Aviv Israel*

ARTICLE INFO

*Article history:*
Received 13 July 2015
Received in revised form
11 October 2015
Accepted 16 October 2015
Available online 23 October 2015

*Keywords:*
Detector
Simulation
Edge-effect
CdZnTe

ABSTRACT

Current increase due to edge effect in ohmic contacts was calculated by finite-element software in three-dimensional devices. The emphasis in this study is on semi-intrinsic (SI) and compensated high resistivity semiconductors. It was found that the enhanced electric field around the contact edges may cause about twofold increase in the total contact current. For contact radii larger than the device thickness and nano scale contacts the impact is considerably reduced. In nanoscale contacts the edge effect does not control the electric field under the entire contact, but rather decreases. The introduction of velocity saturation model has a limited impact, and only in compensated semiconductors.



## 1. Introduction

Applications of high resistivity (high-ρ) semiconductors are extensively growing. Traditionally integrated electronics utilized low resistivity semiconductors, and the high-ρ niche was limited to such applications as radiation detectors, etc. [1–4]. However, recently integration of RF circuits with on-chip antennas, and other applications, including microwave and Terahertz devices, introduced the high-ρ semiconductors into more and more fields [5–8]. In addition it is well known that even extrinsic moderate resistivity semiconductor (e.g., silicon, silicon–germanium, etc.) may become high-resistivity (and also invert the conductivity type) after irradiation. This study uses wide bandgap II–VI alloy for calculations, but the results are generic and can be adapted to other materials. Cadmium–zinc–telluride ($Cd_{1-x}Zn_xTe$) is a family of ternary semiconductors with very promising features: wide band-gap (1.5–2.26 eV), high average atomic number (~50), and reasonably high carrier mobilities ($\mu_n \sim 1000$, $\mu_p \sim 80\ cm^2\ V^{-1}\ s^{-1}$). The resistivity of the alloy may be very high (e.g., above $10^{10}\ \Omega\ cm$ for $x=0.15$), which approaches the intrinsic limit. This is not easily explained due to the high concentrations of impurities and structural defects in the alloys. To obtain such high resistivity the crystals manufacturers often intentionally introduce dopant impurities with shallow energy levels and high concentrations (e.g., indium with a concentration, $N_D$, of $\sim 10^{16}\ cm^{-3}$); yet in $Cd_{0.85}Zn_{0.15}Te$ with $\rho = 10^{10}\ \Omega\ cm$ at thermo-dynamic equilibrium (TDE) the expected free electron concentration, $[e_{TDE}]$, is about $6.1 \times 10^5\ cm^{-3}$ (for a typical value of $\mu_e = 1000\ cm^2\ V^{-1}\ s^{-1}$). Such high resistivity of the raw material without its high purity and perfection can most likely be explained by deep-level compensation [9,10]. Contacts to high resistivity semiconductors in general, and compensated semiconductors in particular, are very challenging in both, implementation and modeling. In recent years there is an ongoing effort to model ohmic and Schottky contacts to such materials [11–13]. For ohmic contacts simple modeling is only valid under overwhelmingly simplifying assumptions (e.g., infinite contacts, constant carrier mobilities, etc.).

Various aspects of ohmic contact downscaling, such as total current dependence on the bias, and carrier depletion/accumulation under velocity saturation conditions, were discussed in Ref. [13]. In high-resistivity semiconductors it was shown that in presence of velocity saturation below certain contact size the current–voltage curves become non-linear and even asymmetric [13]. This is true, for both, semi-intrinsic and compensated semiconductors. The current article focuses on the radial current distribution in ohmic contacts under downscaling. Specifically, its goal is estimating the impact of the edge effect on the total contact current under scaling.

## 2. Simulation results and discussion

The calculations were performed using state-of-the-art Sentaurus software packet [14]. The finite element program was used to solve Poisson and continuity equations over a three-dimensional grid. A novel II–VI alloy semiconductor was introduced into its library using data available for $Cd_{1-x}Zn_xTe$ with $x \sim 0.15$ (carrier mobilities, bandgap, effective masses, etc.) [10]. In addition, the Caughey and Thomas velocity saturation model

http://dx.doi.org/10.1016/j.nima.2015.10.063
0168-9002/

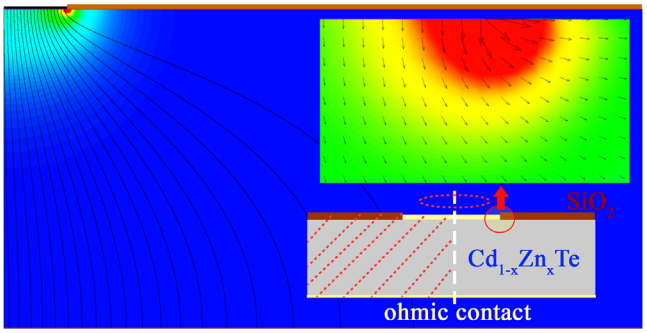


**Fig. 1.** Radial cut (from the center to the edge) of a cylindrical device with a 100 μm radius contact, including current density streamlines at +100 V bias. The colors represent the amplitude of current density (0–2 μA/cm$^2$ range). The bottom inset shows center cut with regions. The upper inset zooms on the contact edge region with current density vectors. (For interpretation of the references to color in this figure legend, the reader is referred to the web version of this article.)

(often referred as the Canali model) was adopted from the silicon model [15]:

$$\mu(E)=\mu_0\left[1+\left(\frac{\mu_0 E}{v_{Sat}}\right)^{\beta}\right]^{-\frac{1}{\beta}} \text{ or } v(E)=\mu_0 E\left[1+\left(\frac{E}{E_C}\right)^{\beta}\right]^{-\frac{1}{\beta}} \quad (1)$$

were $\mu$(E) and $v$(E) are the modified carrier mobility and velocity, respectively; $\mu_0$ is the mobility at low electric fields, $E$ is the local electric field intensity, $v_{Sat}$ is the saturation velocity, and $E_C$ is the critical electric field, $E_C=v_{Sat}/\mu_0$.

Disk shape substrates with a thickness of 500 μm and radii of 1 and 20 mm were used in calculations. The contact radii were downscaled from 20 mm (full size) to 10 nm, with field oxide passivation around the contacts. Radial cut of such device with a 100 μm radius contact is shown in Fig. 1. The main figure features the electric field (E-field) intensity and field lines, the upper inset shows the current vectors around the contact edge, and the bottom inset schematically shows the drawn region of the device. All high resistivity $Cd_{1-x}Zn_xTe$ crystals in this study have 1.6 eV bandgap (corresponding to $x\sim0.15$), and resistivity of $10^{10}$ Ω cm. To obtain such resistivity in semi-intrinsic (SI) samples $N_D$ was set to $6.02\times10^5$ cm$^{-3}$ (to yield $[e]\approx6.13\times10^5$ cm$^{-3}$, and $\rho\approx10^{10}$ Ω cm); in compensated material shallow level acceptor concentration was set to $N_A=10^{16}$ cm$^{-3}$, (as typical indium concentration intentionally introduced during the crystal growth process [16]), and deep level donors $N_{DD}=5\times10^{18}$ cm$^{-3}$ at $E_{DD}=E_V+0.72$ eV [10]. Under TDE conditions all semi-intrinsic and deep level compensated samples have the same resistivity. Ideal ohmic contacts are defined by "flat-band" interface conditions at TDE (implying equal bulk and interface carrier concentrations, $[e,h]^S_{TDE}=[e,h]^B_{TDE}$), and infinite recombination velocities (ensuring that the condition $[e,h]^S=[e,h]^B_{TDE}$ is valid under bias as well). For such ideal ohmic contacts and constant carrier mobilities in the bulk ("bulk mobilitiesflat-band") the electric field (E-field) distribution and carrier concentrations are very similar in SI and compensated samples (with slight deviation in small contacts as discussed below). However, when carriers' velocity saturations in the bulk are accounted for (namely, $\mu^B_{e,h}=f(E)$), the impact of the deep donors on internal E-field distribution becomes imperative. Under the bias the occupancies of the deep donors are determined by their capture cross-sections and free carrier concentrations, thus, even moderate carrier density variations may cause dramatic space charge perturbations. Four different cross-section sets were defined for the deep donors: HH ($\sigma_e=\sigma_h=10^{-13}$ cm$^2$), LL ($\sigma_e=\sigma_h=10^{-20}$ cm$^2$), HL ($\sigma_h=10^{-13}$ cm$^2$, $\sigma_e=10^{-20}$ cm$^2$), LH ($\sigma_h=10^{-20}$ cm$^2$, $\sigma_e=10^{-13}$ cm$^2$), where H and L define "high" and "low" cross-sections values, respectively.

It should be noted that ideal ohmic contact definition sets only the *interface* conditions, however it is usually assumed that under

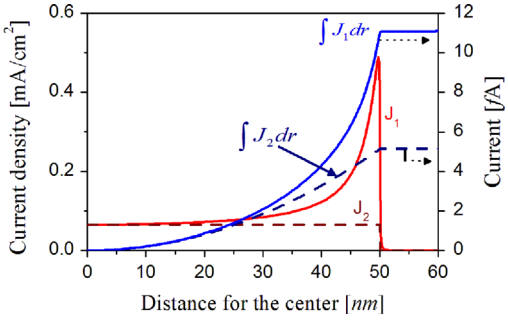


**Fig. 2.** Radial distributions of the current densities and their integrals for a 50 nm radius ohmic contact on SI bulk with $\rho=10^{10}$ Ω cm. Curve $J_1$ represents the calculated current density, and curve $J_2$ the center current density distributed uniformly over the contact.

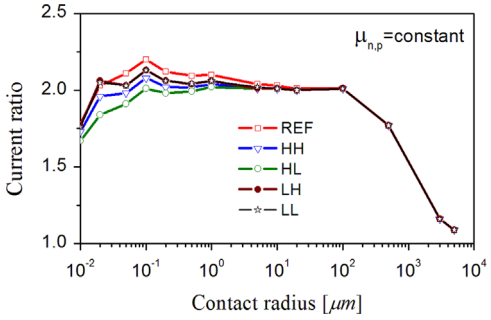


**Fig. 3.** The total calculated contact currents normalized to their corresponding "edgeless cases" (uniform current density under the contact), namely, $\int J_1/\int J_2$ ratios from Fig. 2, illustrating the impact of the edge effect at various contact radii.

ideal ohmic contacts the carrier concentration profiles in the semiconductor are uniform and TDE values are: $[e,h]^S=[e,h]^B=[e,h]^B_{TDE}$. This is not a valid approximation for high E-fields, high resistivity semiconductors (SI or compensated), or when carrier velocities saturate. In this case all mentioned factors may be applied. The E-field line density around the contact edges is higher compared to the contact center, thus, higher current density under the contact edge is expected (the main aspect of the "edge-effect"). The non-uniform E-field distribution may also cause "second order" effects (e.g., local heating, enhanced tunneling, Poole–Frenkel effect, etc.) that are not in the scope of this study. The question what is the extra *drift-diffusion* current ("first order effect") added due to the "edge-effect" is not trivial, particularly in high-resistivity semiconductors. To address this issue vector components of the current density were calculated along the radial axis under the contacts. The amplitude of the vector component normal to a front 50 nm radius contact on SI material at +5 V bias is denoted $J_1$ in Fig. 2. The current density component exhibits a noticeable peak near the edge. For comparison, curve $J_2$ represents uniform (center value) current density. The radial integration of the constant current density ($J_2$) yields the expected $r^2$ dependence, whereas its comparison to the radial integration of the "real" calculated current shows the edge impact. For the 50 nm radius the current increase due to the edge effect is approximately twofold. In the assumption of a constant mobility the results for positive and negative bias polarities are rather similar.

The ratios of the total contact currents with the edge-effect taken into account relative to the current in the case of "no edge effect" calculated for the bias voltage of +5 V and in the assumption of constant mobilities are shown in Fig. 3. For large contact radii (compared to the device thickness) the ratio of the E-field at the edge to that at the center is very high; however the fraction of the area with high E-field to the total contact area is negligible, thus, in such contacts the current increase due to the